

Biexciton binding energy in parabolic GaAs quantum dots

著者別名	舛本 泰章
journal or publication title	Physical review B
volume	73
number	12
page range	125321
year	2006-03
権利	(C)2006 The American Physical Society
URL	http://hdl.handle.net/2241/98237

doi: 10.1103/PhysRevB.73.125321

Biexciton binding energy in parabolic GaAs quantum dots

Michio Ikezawa,¹ Selvakumar V. Nair,² Hong-Wen Ren,^{1,*} Yasuaki Masumoto,¹ and Harry Ruda²

¹*Institute of Physics, University of Tsukuba, Tsukuba 305-8571, Japan*

²*Centre for Nanotechnology, University of Toronto, Toronto M5S 3E3, Canada*

(Received 20 October 2005; revised manuscript received 17 January 2006; published 17 March 2006)

Biexcitons confined in parabolic quantum dots are investigated both experimentally and theoretically. A biexcitonic beat is observed by using time-resolved four-wave mixing in strain-induced GaAs quantum dots formed in the quantum well. The period of the beat is about 1.5 times shorter than that from the quantum well region in the same well. The shortening of the beat period is direct evidence of an increase in the biexciton binding energy in the quantum dots due to the lateral confinement induced by the stressors. Magnetic field dependence of the biexciton binding energy is investigated, and is found to be almost independent of the external magnetic field up to 8 T. A theoretical calculation of the biexciton binding energy is presented to explain the observed magnetic field dependence.

DOI: [10.1103/PhysRevB.73.125321](https://doi.org/10.1103/PhysRevB.73.125321)

PACS number(s): 78.47.+p, 78.67.Hc

I. INTRODUCTION

Physics of excitons and excitonic complexes such as biexcitons, charged excitons, and triexcitons confined in low-dimensional quantum structures has been a subject of intensive study in recent years. In addition to interest of basic physics, these studies are driven by the need for a deep understanding of such confined states for the successful application of quantum structures to quantum information technologies. The binding energy of an excitonic complex in nanostructures is expected to be enhanced compared to the bulk material due to the spatial confinement of electrons and holes. Actually, in many kinds of quantum dots (QD) such as Stranski-Krastanov grown dots or dots dispersed in glass matrices, large binding energy of biexcitons has been reported.¹ Large binding energy of the biexciton state is particularly important in light of the recent demonstration of the ability to operate a two-qubit gate using exciton and biexciton states.²

General considerations point to a strong dependence of the enhancement of the biexciton binding energy on dimensionality. It is well known that the biexcitons localized in potential minima originating from well width fluctuations or alloy fluctuations have larger binding energy compared to that of an ideal quantum well (QW).³⁻⁸ Although these examples demonstrate the enhancement of the biexciton binding energy in reduced dimensionality, the additional lateral confinement potential in these cases is naturally formed and is, therefore, unknown and uncontrollable. For a better understanding of the effect of dimensionality and confinement, it is desirable to study a system with a well-defined confinement potential that could be easily controlled. Strain-induced quantum dots (SIQDs) that are formed in a buried QW by the stress modulation arising from self-assembled islands fabricated on the surface⁹ provide such an ideal system. Carriers in SIQDs are confined laterally in the QW by an almost parabolic potential with no defect at the surface, resulting in nearly equally spaced energy levels, which greatly simplifies theoretical treatment. In contrast to other kinds of QDs, the confinement potentials could be finely controlled in SIQDs by changing the QW and spacer widths⁹ with monolayer pre-

cision provided by epitaxial growth. Furthermore, as QW and QD coexist inherently in a SIQD sample, we can observe the effect of the additional lateral confinement within the same quantum well. In addition, as the confinement potential is rather deep, QW and SIQD are energetically well separated, which enables us to apply the quantum beat technique using ultrafast laser pulses to measure the binding energy in QW and in SIQD separately.

In this paper we report transient four-wave mixing (FWM) in a strain-induced GaAs QD measured by a highly sensitive heterodyne FWM technique. Using this technique, we detected the biexcitonic quantum beat that is related to the biexciton binding energy in the SIQD. We also present the measurement and theoretical calculation of the magnetic field dependence of the biexciton binding energy.

II. EXPERIMENTAL DETAILS

The structure of the sample studied is depicted in Fig. 1(a). The SIQDs were formed in a single GaAs/Al_{0.3}Ga_{0.7}As QW of 3.8 nm in width using InP stressors of 90 nm in diameter. The areal density of the stressor was $3 \times 10^9/\text{cm}^2$. The width of the Al_{0.3}Ga_{0.7}As barrier on the QW is 9.0 nm. The photoluminescence (PL) spectrum of the sample is shown in the right part of the figure. The weak peak centered at 1.647 eV is due to PL from the GaAs QW, while the intense peak centered at 1.600 eV originates from the GaAs SIQDs, showing a confinement potential of 47 meV. The energy separation between the lowest state and the first excited state was measured by PL excitation spectroscopy as 16 meV. The detection method employed in this study is based on Refs. 10 and 11. Recently, a very similar method was successfully utilized to investigate the biexciton binding energy in annealed In_xGa_{1-x}As QDs.¹² We have modified the method for reflection geometry. The excitation laser was a mode-locked femtosecond Ti:sapphire oscillator with a repetition rate of 80 MHz, and a typical pulse width of 100 fs. The output beam was divided into three beams, and two of them were frequency-shifted by acousto-optic modulators to $\nu + 110$ MHz and $\nu + 111$ MHz, respectively, where ν is the

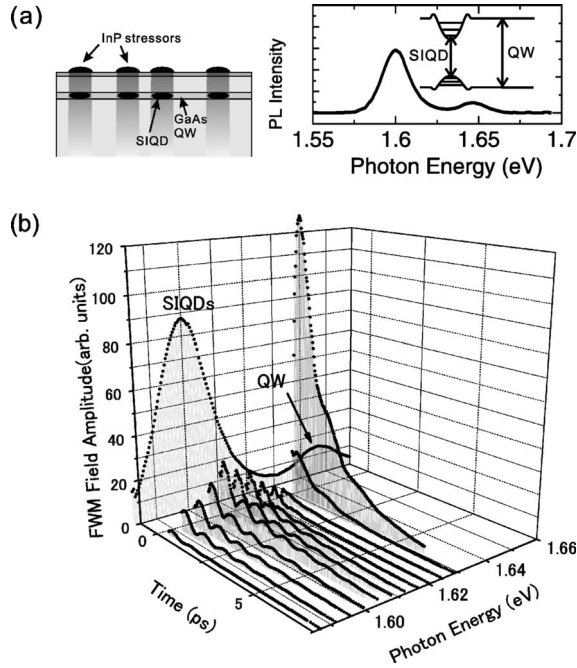


FIG. 1. (a) The structure of the strain-induced GaAs quantum dots and PL spectrum at 2 K. The shades schematically represent strain fields due to InP stressors. (b) FWM signals excited by various photon energies at 20 K. For this measurement, the spectral width of the laser was reduced to 15 meV.

optical frequency. The very weak FWM signal with a frequency of $\nu+220$ MHz induced by the two sequential pulses, the first one (ν) and the second one ($\nu+110$ MHz) delayed by τ , was overlapped with the other strong beam ($\nu+111$ MHz) via a beamsplitter, and detected by balanced PIN photodiodes. The interference component at $(\nu+220 \text{ MHz}) - (\nu+111 \text{ MHz}) = 109$ MHz was extracted by a spectrum analyzer. One of the beams was intensity modulated by an optical chopper, and a lock-in detection was utilized. The sensitivity of this system was found to be sufficient to detect the FWM from a single layer of QDs.

III. RESULTS AND DISCUSSION

In Fig. 1(b), the time-integrated FWM signals measured at 20 K are shown as a function of the center photon energy of the excitation laser. The PL spectrum is plotted in a vertical plane for comparison. When the excitation photon energy is at the center of the PL peak of QW, a quite strong FWM signal was observed (not shown). The signal decreases rapidly with decreasing photon energy, and then increases as the energy approaches the SIQDs peak. After the laser photon energy passes through the PL band, the signal fades out. Therefore, it is confirmed that the signal near the SIQDs peak originated from the lowest state in SIQDs. As it appears at first glance, the signals have a pronounced beat structure, which is not clear in the signal from the QW.

The FWM signals measured at the center of QW peak and SIQDs peak at 2 K are shown in Fig. 2. Except for the beat structure, the intensity of the FWM signal decays almost exponentially. The decay time constants for the QW and

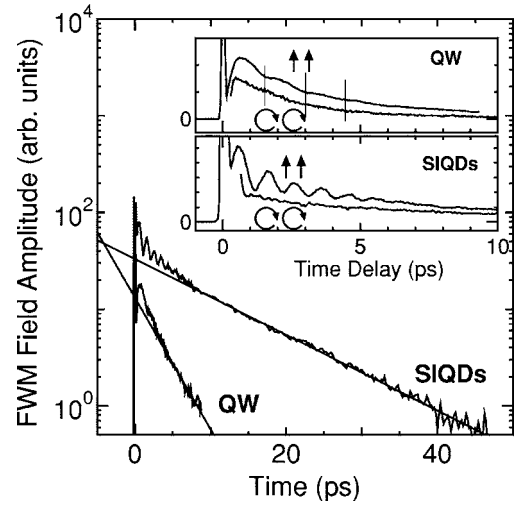


FIG. 2. The logarithmic plot of the FWM signal at the SIQDs peak and at the QW peak at 2 K. The decay time of the signal at SIQDs (QW) is 12 ps (3.2 ps). Inset: The polarization dependence of the FWM signal of the initial part.

SIQDs differed from each other, and were independent of the excitation laser power under the present experimental conditions. The dephasing time was determined to be 24 ps for excitons in SIQDs.¹³ Polarization dependence was investigated in order to discuss the origin of the beat structures. A clear oscillation with a period of 1 ps was observed for the SIQDs when the two excitation pulses have collinear polarization, while it disappeared when the pulses were cocircularly polarized, as shown in the inset. The polarization dependence of the beat strongly suggests that the biexciton is the origin of the beat, as biexcitons consist of two excitons of opposite spin, and therefore cannot be excited by cocircular polarized pulses.¹⁴ The same is true for the signal from the QW. The difference in the beat periods would therefore represent an enhancement of the biexciton binding energy in SIQDs. In the present sample, the binding energy increases from 2.8 to 4.1 meV, corresponding to an enhancement factor of 1.5. We found that the enhancement factor had a tendency to decrease with decreasing the lateral confinement potential: 1.45 for 44 meV, 1.3 for 36 meV. It seems reasonable to suppose that the biexciton in QW is not localized but free in the present sample, because a theoretical calculation¹⁵ that includes localization of biexciton shows that the localized biexciton in 3.8 nm QW should have much larger binding energy, and the experimental results cited in the paper also support this assumption.

Next, we measured the magnetic field dependence of the biexciton binding energy in Faraday geometry (Fig. 3). With increasing the magnetic field, another beat structure emerged, and it modified the biexcitonic beat. The frequency of the slow beat depends linearly on the magnetic field [see Fig. 3(b), inset]. This beat is assigned to the quantum beat between the right-circularly polarized exciton and left-circularly polarized exciton separated by the Zeeman splitting. The g factor of excitons in the SIQDs is deduced to be 0.64, and agrees well with that measured by polarized time-resolved luminescence.¹⁶ Turning now to the biexcitonic beat, the beat frequency and corresponding binding energy

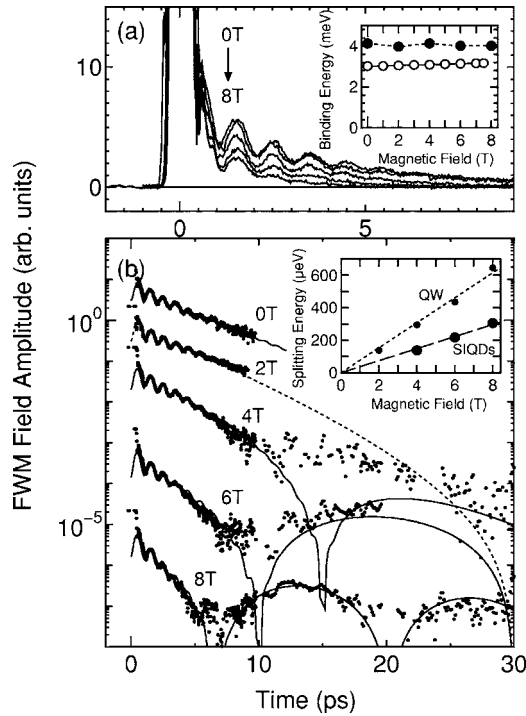


FIG. 3. Magnetic field dependence of the biexcitonic beat (a) and slow beat (b). The biexcitonic beat remains constant up to 8 T. The open circles in the inset represent the result of the theoretical calculation (see the text). The slow beat results from the Zeeman splitting of excitons in SIQDs. The g factor of excitons in SIQDs is deduced as 0.64, while that in QW is 1.3.

show practically no change up to a magnetic field of 8 T, as shown in Fig. 3(a).¹⁷ Similar weak dependence on the magnetic field was also reported for the biexciton binding energy in InGaAs QW, but no explanation was given.¹⁸ The weak magnetic field dependence is not caused by the weakness of the magnetic confinement compared to that due to the strain field. It could be understood by theoretical considerations described below.

We calculated the exciton and biexciton states in SIQDs using a configuration interaction approach.^{19,20} For single particle electron and hole states, we use a two band effective mass approximation with an isotropic electron band and an anisotropic hole band. Previous theoretical calculations have established that single particle SIQDs could be well described by such a model.²¹ Further, we explicitly make use of the cylindrical symmetry of the confining potential in SIQDs. In this approximation, the hole single particle Hamiltonian, \mathcal{H}_h , for a given axial angular momentum l_h takes the form

$$\mathcal{H}_h = E_v + \frac{\hbar^2}{2} \left(\frac{1}{r_h} \frac{\partial}{\partial r_h} r_h \frac{\partial}{\partial r_h} + \frac{\partial}{\partial z_h} \frac{1}{m_h^{\parallel}} \frac{\partial}{\partial z_h} - \frac{l_h^2}{m_h^{\perp} r_h^2} \right) + V_h(r_h, z_h), \quad (1)$$

where m_h^{\parallel} and m_h^{\perp} denote the hole effective masses along the z direction and in the x - y plane, respectively. Both the electron and hole effective masses could be position dependent. The confining potential $V_h(r, z)$ is determined by the band edge discontinuities and the strain distribution induced by

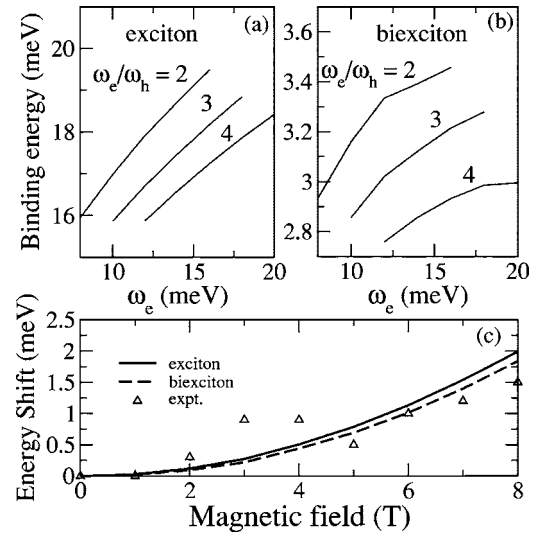


FIG. 4. Calculated binding energies of (a) exciton and (b) biexciton for various values of the confinement parameters ω_e and ω_h (see the text for details). The bottom panel (c) shows the magnetic field dependence of the exciton (solid line) and biexciton (dashed line) emission energies for $\omega_e = 12$ meV and $\omega_h = 4$ meV. The points (open triangles) denote experimental data for the exciton.

the stressor and $E_{c(v)}$ is the conduction (valence) band edge of the barrier material. A similar equation holds for the electron.

Although mixing of heavy-hole (HH) and light-hole (LH) bands is known to affect excitons and biexciton states, the single hole-band model used here is a good approximation. In the quantum well, the HH-LH splitting due to confinement is about 35 meV and, based on early calculations,²² we estimate that the HH-LH mixing would change the exciton binding energy by less than 10% (1 meV). In the quantum dot, the band mixing effects would be even weaker because of increased HH-LH splitting due to the stressor-induced strain. From continuum elasticity calculations, we find that, at the location of the quantum well, which is about 11 nm below the stressor, the biaxial strain increases the HH-LH splitting by an additional 15 meV.

We calculated the single particle energies and envelope functions using a finite difference discretization of \mathcal{H}_e and \mathcal{H}_h in the r - z plane. While the confining potentials $V(r, z)$ could be directly related to the structure of the QD, there is considerable uncertainty in the resulting potentials due to inaccuracies in the known values of deformation potentials and elastic constants. Here we have opted to use a phenomenological confinement potential given by $V_{e(h)}(r, z) = E_{e(h)}(r, z) \pm m_{e(h)}^{\perp} \omega_{e(h)}^2 r^2 / 2$, where $E_{e(h)}$ describes the band edge discontinuities relative to the conduction (valence) band edges of the barrier and ω_e and ω_h are treated as parameters. Once the single particle states are determined, we construct biexciton states within a CI approach.²⁰ The Coulomb interaction is screened by the bulk dielectric constant of GaAs. We use as high as 50 single particle states leading to more than 10^5 configurations, which is much larger than previous calculations (see Ref. 23).

Finally, in the presence of a magnetic field (\mathbf{H}) the single particle Hamiltonian is modified by replacing $-i\nabla$ by

$-i\nabla \pm (e/\hbar c) A$, where the + sign applies to electrons and the – sign to holes and $A = (\mathbf{H} \times \mathbf{r})/2$. All results reported here are for the magnetic field along the z direction.

The calculated binding energies and the magnetic field dependence of exciton and biexciton emission energies is shown in Figs. 4(a)–4(c). The data shown in Fig. 4(c) are for $\omega_e = 12$ meV, $\omega_h = 4$ meV, which appears to be most appropriate for our sample.²⁵ The biexciton binding energy, given by the difference between exciton and biexciton emission energies, is shown in the inset of Fig. 3(a) along with the experimental data. The calculated results are in good agreement with the experiment.

The calculated biexciton binding energy for the above parameters is about 3 meV, which is somewhat smaller than the observed value of 4 meV. By a comparison of CI and path-integral-Monte-Carlo methods, we have concluded that even the relatively large basis set used by us may not be enough to obtain well-converged biexciton states in these QDs. This point will be addressed in more detail elsewhere.²⁴

An analysis of the convergence indicates that the calculated weak magnetic field dependence of the biexciton binding energy is not an artifact. In a simple picture one may think that the additional confinement due to the magnetic field will lead to an increase in the binding energy of multiparticle states. In fact, the diamagnetic confinement potential due to a field of 8 T would essentially increase ω_e from 12 to 14.5 meV and ω_h from 4 to 5.6 meV. Considering this effect alone, one would expect the exciton binding energy to increase from 16 to 18 meV, which is indeed in very good agreement with the actual calculated value.

However, the same argument would mean that a field of 8 T should increase the biexciton binding energy from 3 meV to about 3.3 meV, in contradiction with the actual

extremely weak magnetic field dependence. This behavior is intimately related to the fact that, in QDs smaller than the exciton Bohr radius, the exciton binding energy is predominantly determined by the Hartree term or first order perturbation theory and is insensitive to correlations described by excited state contributions. On the other hand, the biexciton binding is completely determined by correlations, and hence by contributions of excited state configurations. The magnetic field causes orbital Zeeman splitting of the excited states and thus reduces the mixing of the ground and excited state configurations. It is this competition between the paramagnetic and diamagnetic terms that leads to a weak dependence of the biexciton binding energy on the magnetic field. Calculations in which the paramagnetic term was artificially switched off confirms this interpretation.

IV. CONCLUSION

The FWM of parabolic GaAs SIQD formed in a GaAs single QW was studied using a highly sensitive heterodyne detection technique. A remarkable enhancement of the biexciton binding energy in SIQD due to the lateral confinement was detected by direct comparison with the QW based on the beating period in the FWM signal. The magnetic field dependence of the binding energy was investigated in Faraday geometry, and was found to be very weak, although the exciton emission energy shows a strong shift with magnetic field. A theoretical calculation using the configuration interaction approach supports this observation.

S.V.N and H.R acknowledge support from NSERC and AFOSR.

*Present address: Applied Optoelectronics Incorporation, 13111 Jess Pirtle Boulevard, Sugar Land, Texas 77478, USA.

- ¹A. D. Yoffe, *Adv. Phys.* **50**, 1 (2001), and references therein.
- ²X. Li, Y. Wu, D. Steel, D. Gammon, T. H. Stievater, D. S. Katzer, D. Park, C. Piermarocchi, and L. J. Sham, *Science* **301**, 809 (2003).
- ³O. Heller, Ph. Lelong, and G. Bastard, *Phys. Rev. B* **56**, 4702 (1997).
- ⁴D. A. Kleinman, *Phys. Rev. B* **28**, 871 (1983).
- ⁵K. Brunner, G. Abstreiter, G. Böhm, G. Tränkle, and G. Weimann, *Phys. Rev. Lett.* **73**, 1138 (1994).
- ⁶F. Kreller, M. Lowisch, J. Puls, and F. Henneberger, *Phys. Rev. Lett.* **75**, 2420 (1995); T. Häuptl, H. Nickolaus, F. Henneberger, and A. Schülzgen, *Phys. Status Solidi B* **194**, 219 (1996).
- ⁷U. Woggon, K. Hild, F. Gindele, W. Langbein, M. Hetterich, M. Grün, and C. Klingshirn, *Phys. Rev. B* **61**, R12632 (2000).
- ⁸W. Langbein and J. M. Hvam, *Phys. Rev. B* **59**, 15405 (1999).
- ⁹H. Lipsanen, M. Sopanen, and J. Ahopelto, *Phys. Rev. B* **51**, R13868 (1995).
- ¹⁰M. Hofmann, S. D. Brorson, J. Mørk, and A. Mecozzi, *Appl. Phys. Lett.* **68**, 3236 (1996); A. Mecozzi, J. Mørk, and M. Hofmann, *Opt. Lett.* **21**, 1017 (1996).
- ¹¹P. Borri, W. Langbein, S. Schneider, U. Woggon, R. L. Sellin, D.

- Ouyang, and D. Bimberg, *Phys. Rev. Lett.* **87**, 157401 (2001).
- ¹²W. Langbein, P. Borri, U. Woggon, V. Stavarache, D. Reuter, and A. D. Wieck, *Phys. Rev. B* **69**, 161301(R) (2004).
- ¹³The dephasing time seems rather short for a zero-dimensional system. However, relatively broad homogeneous widths are reported in InGaAs SIQDs by single dot spectroscopy, and “near surface impurity state” is suggested as an additional dephasing mechanism, because the SIQDs are inherently located near the surface. See, for example, C. Obermüller *et al.*, *Appl. Phys. Lett.* **74**, 3200 (1999).
- ¹⁴T. F. Albrecht, K. Bott, T. Meier, A. Schulze, M. Koch, S. T. Cundiff, J. Feldmann, W. Stolz, P. Thomas, S. W. Koch, and E. O. Göbel, *Phys. Rev. B* **54**, 4436 (1996).
- ¹⁵A. V. Filinov, C. Riva, F. M. Peeters, Yu. E. Lozovik, and M. Bonitz, *Phys. Rev. B* **70**, 035323 (2004).
- ¹⁶K. Nishibayashi, T. Okuno, Y. Masumoto, and H. W. Ren, *Phys. Rev. B* **68**, 035333 (2003).
- ¹⁷The damping constant of the biexcitonic beat appears to decrease with increasing the magnetic field. This feature arises from the Zeeman splitting of exciton states and it does not mean any other biexciton related phenomena such as inhomogeneous broadening of the biexciton binding energy in the magnetic field.
- ¹⁸T. Baars, M. Bayer, A. A. Gorbunov, and A. Forchel, *Phys. Rev.*

- B **63**, 153312(R) (2001).
- ¹⁹L. Bányai and S. W. Koch, *Semiconductor Quantum Dots* (World Scientific, Singapore, 1993).
- ²⁰S. V. Nair, in *Semiconductor Quantum Dots: Physics, Spectroscopy and Applications*, edited by Y. Masumoto and T. Takagahara (Springer-Verlag, Berlin, 2002).
- ²¹J. Tulkki and A. Heinamaki, Phys. Rev. B **52**, R8239 (1995).
- ²²G. D. Sanders and Y-C. Chang, Phys. Rev. B **32**, R5517 (1985); U. Ekenberg and M. Altarelli, *ibid.* **35**, 7585 (1987).
- ²³S. Corni, M. Brasken, M. Lindberg, J. Olsen, and D. Sundholm, Phys. Rev. B **67**, 045313 (2003).
- ²⁴M. Wimmer, S. V. Nair, and J. Shumway, Phys. Rev. B, (to be published).
- ²⁵The PL spectrum shows an excited state emission 16 meV above the ground state. Further, based on strain calculations we estimate the ratio ω_e/ω_h to be close to 3.